Implementing diagnostic Bayesian networks for heat recovery ventilation in real-world scenarios: A Dutch case study

Ankeren, Lars van Koetsveld van; Lu, Chujie; Itard, Laure

DOI
10.1016/j.jobe.2025.113527

Publication date
2025

Document Version
Final published version

Published in
Journal of Building Engineering

Citation (APA)
Ankeren, L. V. K. V., Lu, C., & Itard, L. (in press). Implementing diagnostic Bayesian networks for heat recovery ventilation in real-world scenarios: A Dutch case study. *Journal of Building Engineering*, *111*, Article 113527. https://doi.org/10.1016/j.jobe.2025.113527

Journal of Building Engineering 111 (2025) 113527

Contents lists available at ScienceDirect

Journal of Building Engineering

journal homepage: www.elsevier.com/locate/jobe

Implementing diagnostic Bayesian networks for heat recovery ventilation in real-world scenarios: A Dutch case study

Lars van Koetsveld van Ankeren, Chujie Lu *, Laure Itard

Department of Architectural Engineering and Technology, Faculty of Architecture and the Built Environment, Delft University of Technology, Julianalaan 134, 2628 BL, Delft, the Netherlands

ARTICLE INFO

Keywords:
Diagnostic bayesian networks
Fault detection and diagnosis
Building energy systems
Air handling units
Kafka

ABSTRACT

Fault detection and diagnosis (FDD) are essential for enhancing the performance of heating, ventilation, and air conditioning (HVAC) systems, preventing energy waste, and ensuring indoor comfort. However, popular data-driven FDD approaches encounter challenges, such as the lack of high-quality labeled data, poor generalization, and the black-box nature of the models, which hinder their adoption in the market. Moreover, most existing studies only developed and validated their FDD models in simulation environments or laboratory settings, overlooking practical challenges of operational HVAC systems. First, this study focuses on implementing Diagnosis Bayesian networks (DBNs) in real-world settings, specifically, air handling units with heat recovery wheels in a campus building in the Netherlands. DBNs have been proven to be promising solutions with advantages in interpretability, robustness to uncertainties, and flexibility. Second, a Kafka-based framework is introduced for real-time monitoring in HVAC systems, enabling continuous and scalable data processing. Third, a comprehensive diagnosis analysis is conducted using both historical operational data and experimental fault data. The results reveal significant discrepancies between design documents and the actual operation of the HVAC system, and the DBN successfully identifies eight out of nine injected faults during experimentation. Additionally, the results uncover issues such as false positives due to DBN's limitations, inherent system faults, and unexpected HVAC system behaviors triggered by the simulated faults, offering critical insights into the operational challenges and diagnostic potential of DBNs in real-world HVAC systems. These contributions can advance the practical deployment of interpretable and robust FDD tools in building energy systems.

1. Introduction

In the European Union, approximately 40 % of energy is consumed in buildings, and over one-third of energy-related greenhouse gas emissions come from buildings [1]. The revised Energy Performance of Buildings Directive, entered into force in all EU countries in May 2024, aims to achieve emission reductions of at least 60 % in the building sector by 2030 compared to 2015 and to reach climate neutrality by 2050 [2]. Heating, ventilation, and air conditioning (HVAC) systems, which are crucial for maintaining comfortable and healthy indoor environments, account for the largest share of energy use in buildings [3,4]. However, defects and faults in HVAC systems can lead to unexpected indoor environment conditions and significant energy waste, with estimates suggesting these

* Corresponding author.
E-mail address: c.j.lu@tudelft.nl (C. Lu).

https://doi.org/10.1016/j.jobe.2025.113527
Received 27 February 2025; Received in revised form 2 July 2025; Accepted 20 July 2025
Available online 22 July 2025

Abbreviations

AHU	Air handling unit
ANN	Artificial neural network
BMS	Building management system
CCV	Cooling coil valve
CNN	Convolutional neural network
COP	Coefficient of performance
CPT	Conditional probability table
DBN	Diagnostic Bayesian network
DNN	Deep neural network
DT	Decision tree
FDD	Fault detection and diagnosis
GAN	Generative adversarial network
HCV	Heating coil valve
HCP	Heating coil pump
HRW	Heat recovery wheel
HVAC	Heating, ventilation, and air conditioning
LSTM	Long short-term memory
P&ID	Process and instrumentation diagram
RF	Random forest
RNN	Recurrent neural network
SVM	Support vector machine

Symbols

A_{hcp}	HCP alert
A_{hrw}	HRW alert
$A_{s,fan}$	Supply fan alert
$A_{s,filter}$	Supply filter alert
$A_{r,fan}$	Return fan alert
$A_{r,filter}$	Return filter alert
F	Fault
p	Number of samples in a period
P_s	Supply air pressure
$P_{s,set}$	Supply air pressure setpoint
P_r	Return air pressure
$P_{r,set}$	Return air pressure setpoint
S	Symptom
T_e	Exhaust air temperature
T_i	Inlet air temperature
T_o	Outdoor air temperature
T_p	Preheated air temperature
T_s	Supply air temperature
T_{set}	Supply air temperature setpoint
T_r	Return air temperature
ΔP_s	Pressure difference between supply filter
ΔP_r	Pressure difference between return filter
U_{hcv}	HCV control signal
U_{hrw}	HRW control signal
$U_{s,fan}$	Supply fan control signal
$U_{r,fan}$	Return fan control signal
ε	Threshold

inefficiencies could result in energy losses exceeding 30 % [5,6]. Therefore, fault detection and diagnosis (FDD) play a crucial role in improving HVAC system performance, preventing energy waste, and ensuring indoor comfort.

FDD has been the subject of extensive research, but a disjunction remains between academia and the building industry. FDD approaches can broadly be categorized into two types: knowledge-based and data-driven. Over the past decade, the emergence of artificial intelligence has sparked a surge in interest towards data-driven FDD approaches, which account for approximately 70 % of all related publications [7–9]. These approaches leverage statistical analysis and machine learning models to automatically identify faulty

patterns from data, often achieving high diagnostic accuracy [10]. Despite this academic enthusiasm, the adoption of data-driven FDD in the building industry has been sluggish. An interview conducted by Heimar Anderson et al. [11], which involved interviews with 29 industry experts, revealed that FDD is still largely perceived as an academic concept. The experts indicated unfamiliarity with data-driven FDD approaches, and the market continues to rely heavily on traditional knowledge-based expert systems for diagnosing HVAC system faults. Frank et al. [12] also mentioned that the rule-based FDD approach is the most common FDD approach for large commercial buildings in the US. One primary reason for this slow adaptation is the lack of high-quality labeled faulty datasets for model training, which can be very time-consuming and labor-intensive to determine the actual operating condition or label of each data sample in practice [13]. Another major reason is that each HVAC system has its own unique boundary conditions, such as layout, weather, occupancy, and internal heat gains [14]. Consequently, data-driven FDD approaches encounter challenges related to scalability and transferability, which limit their effectiveness across diverse systems and buildings [8]. Additionally, for market-oriented FDD products, their trustworthiness and interpretability are crucial. The diagnostic mechanisms of data-driven FDD approaches, often viewed as black-box models, can lead to skepticism regarding their reliability and understanding [15].

To address these challenges, diagnostic Bayesian networks (DBNs) offer a promising solution [16,17]. One of the advantages of DBNs is their alignment with HVAC design and implementation practices, providing strong model interpretability and robustness to uncertainties [18]. In DBNs, nodes represent potential faults and related symptoms, while the graphical structure illustrates the relationships between them. The strength of these relationships is quantified using conditional probabilities, providing a transparent and quantitative understanding of how specific faults manifest as symptoms. Furthermore, DBNs are highly flexible in their construction. They can be built using a knowledge-based approach [19–24], which leverages expert insights and domain-specific rules, or through data-driven approaches [25,26], where the graphical structures and probabilities can be learned directly from experimental fault data. Hybrid approaches have also been implemented for DBN construction [27–29], combining both expert knowledge and data-driven learning. This flexibility allows for the integration of multiple information sources, enhancing FDD accuracy and robustness across various application scenarios in buildings.

Although extensive research has been conducted to develop and implement different FDD approaches for building systems, many

Table 1
Related studies on FDD for building energy systems.

Ref.	Year	Objective	Method	Type
[43]	2019	AHU system for an office building	DNN	Simulation
[44]	2020	Multi-zone HVAC system	Auto-associative neural network-based validation	Simulation
[45]	2020	Chiller (ASHARE RP-1043)	GAN	Experimental
[46]	2020	Demand-controlled ventilation	DBN	Case
[22]	2020	HVAC system for a university building	DBN	Case
[23]	2020	HVAC system for a university building	DBN	Case
[47]	2021	Chiller (ASHARE RP-1043)	CNN	Experimental
[26]	2021	Chiller (ASHARE RP-1043)	Reference model-based and faulty data-driven hybrid DBN	Experimental
[27]	2021	AHUs (ASHARE RP-1312)	Knowledge-guided and data-driven DBN	Experimental
[48]	2021	AHUs	Deep RNN	Experimental
[49]	2021	AHUs (ASHARE RP-1312)	Semi-supervised ANN	Experimental
[50]	2021	AHUs for an academic building	Ontological reasoning	Case/Implementation
[16]	2022	AHUs for an industrial building	Object oriented DBN	Case
[40]	2022	HVAC system for a campus building	Discrete DBN	Case
[51]	2022	AHUs	Transformer	Case
[52]	2022	AHUs (ASHARE RP-1312)	RF, SVM	Simulation/ Experimental
[53]	2022	Chiller (ASHARE RP-1043)	Variational autoencoder-based GAN	Experimental
[54]	2023	Multi-zone HVAC system	Bilinear deep Koopman model	Simulation
[55]	2023	Central chilled-water plant	ResNet and VGG	Simulation
[56]	2023	Central chilled-water plant	ResNet and VGG in a knowledge distillation framework	Simulation
[57]	2023	AHUs (ASHARE RP-1312)	Transformer integrated Wasserstein GAN	Experimental
[58]	2023	AHUs (ASHARE RP-1312)	Siamese networks with LSTM	Experimental
[59]	2023	AHUs (ASHARE RP-1312)	BP-MTN	Experimental
[29]	2023	Chiller (ASHARE RP-1043)	Residual–knowledge–data driven DBN	Experimental
[60]	2023	Chiller (ASHARE RP-1043)	Hybrid resampling based improved extreme learning machine	Experimental
[61]	2023	Chiller (ASHARE RP-1043), screw chiller	Knowledge-infused neural network	Experimental
[39]	2023	HVAC system for an experimental facility	Statistical techniques based on Tukey and Relative Entropy statistics	Implementation
[62]	2023	HVAC system for upper secondary schools	DBN, ANN and SVM	Implementation
[63]	2024	HVAC system for a commercial building	Entropy-based DBN	Simulation
[64]	2024	HVAC system for a light commercial building	Decision tree	Case
[28]	2024	Chiller (ASHARE RP-1043)	Data and knowledge fusion-driven DBN	Experimental
[65]	2024	Chiller (ASHARE RP-1043)	DBN with feature selection based on generic algorithm	Experimental
[66]	2024	Chiller (ASHARE RP-1043)	Improved GAN with an enhanced deep extreme learning machine	Experimental
[67]	2024	AHUs (ASHARE RP-1312)	Global modelling scheme integrated dynamic kernel canonical variate analysis	Experimental
[68]	2024	HVAC system for an office building	DBN	Simulation/Case

studies have primarily focused on developing or validating their algorithms in simulation environments, or in laboratory settings [8]. Research on online and real-time implementations of FDD methods in actual buildings is insufficient. In real-world building cases, several practical challenges hinder effective implementation, including a lack of sensors [30,31], poor sensor accuracy and missing sensor values [32–34], non-standardized sensor installations [35], unexpected control logics, inconsistent definitions of Application Programming Interfaces (APIs) [36–38], and real-time data stream processing [39]. These issues significantly limit the practical applicability of FDD methods, underscoring the critical need to address challenges in their on-site implementation.

Furthermore, air handling units (AHUs) are one of the most common and important HVAC systems in buildings. While several studies have successfully developed DBNs for AHUs [19,20,27,40], these efforts have predominantly relied on experimental fault datasets from ASHRAE RP-1312 [41], which focus on AHUs with mixing air chambers commonly used in the U.S. and Asia. However, these AHUs have the potential risk of virus transmission. In contrast, AHUs in Europe typically use heat recovery devices, such as heat recovery wheels (HRWs), with a net physical air separation between the return and supply side, reducing the risk of contamination [42]. Despite the importance of AHUs with these heat recovery systems for safer and healthier ventilation, especially in the post-COVID era, their FDD has not been adequately investigated.

This study aims to bridge the gap between laboratory-based FDD research and real-world applications, offering insights into practical challenges and solutions for FDD in operational buildings. The contributions of this study are summarized as follows.

- A DBN-based FDD approach is developed based on the four symptoms and three faults (4S3F) reference architecture for heating recovery ventilation in a campus building, where AHUs with HRWs is a common system in Europe but under investigated in the context of fault diagnosis.
- A Kafka-based data stream framework is introduced for FDD in HVAC systems, enabling real-time, continuous, and scalable data acquisition, storage, and processing.
- A comprehensive diagnosis analysis is conducted using both historical operational data and experimental fault data.
- Critical insights are provided into the operational challenges and diagnostic potential of DBNs in real-world HVAC systems.

The rest of this paper is organized as follows. Section 2 presents a literature review of FDD in building energy systems. Section 3 introduces the theoretical fundamentals of DBNs, the 4S3F reference architecture, and the Kafka-based FDD framework in buildings. Section 4 describes the case building and the proposed DBN. Section 5 presents the diagnostic analysis performed on historical data and experimental data. Section 6 concludes the key findings of this study, discusses its limitations, and suggests directions for future studies.

2. Literature review

This section reviews the relevant studies on FDD in building energy systems, which can be divided into four categories: simulation, experimental, case, and implementation studies [11]. Typically, simulation and experimental studies have primarily focused on the development of FDD methods, while case and implementation studies focused on evaluating the capabilities of the various FDD methods in real-world buildings. Table 1 summarizes the related studies on FDD for building energy systems in the last five years.

In simulation studies, labeled fault data used for model training, testing, and validation are generated through simulation environments. The simulation can precisely control the data resolution as needed, and there are no issues with data quality, missing values, or measurement uncertainty. Lee et al. [43] produced fault operational data of a 10-floor office building in EnergyPlus and developed a deep neural network (DNN) to diagnose the faults in AHU systems. Elnour et al. [44] obtained fault-free data in a 3-zone HVAC system using TRNSYS and proposed an auto-associative neural network-based method to validate and diagnose sensor faults. Huang et al. [63] generated the fault data of a virtual HVAC system testbed developed using Modelica in Dymola environment and evaluated the effectiveness of a novel entropy-based causality learning framework for DBN. Gao et al. [68] created a digital twin model for a building based on IDA-ICE and implemented DBN to diagnose faults. Gao et al. [55,56] utilized a Python-based simulation program to collect fault operational data of a central chilled-water plant, and they analyzed the performance of pruning and knowledge distillation of deep learning models. However, well-validated FDD models using simulated data may not always perform effectively when applied to real-world buildings, even though the simulations are carefully developed and calibrated. Huang et al. [52] found distribution differences between AHU fault data simulated by HVACSIM+ and real building data, resulting in FDD models trained on simulated data failing to generalize well when applied to real-world building data.

In experimental studies, labeled fault data are typically emulated in controlled laboratory settings, where sensors are properly calibrated to ensure high-quality data with few missing values. The severity of faults can also be carefully controlled in these experiments. Most of the experimental studies rely on fault datasets from the ASHRAE RP-1312 [41] and RP-1043 projects [69], which focus on AHUs and chillers, respectively. The models commonly used in these studies include random forest (RF) [52], support vector machine (SVM) [52], back propagation multi-dimensional Taylor network (BP-MTN) [59], artificial neural network (ANN) [49], convolutional neural network (CNN), Recurrent neural network (RNN) [48], long short-term memory (LSTM) [58], generative adversarial network (GAN) [45,53,57,66], Transformer [57], and DBN [26–29,40,65]. Both simulation and experimental studies offer ideal conditions for developing and evaluating FDD models. While experimental studies offer a relatively realistic setting, they are often costly, time-consuming, and limited in the types of faults they can emulate. Additionally, they still may not fully capture the complexities of FDD tasks in real-world buildings.

In case and implementation studies, data are obtained in actual measurement campaigns or directly sourced from building management systems (BMS) in real-world buildings, which brings many practical challenges. Firstly, data resolution may be difficult to

adjust if sourced from BMS records. Data quality is often inconsistent, with significant amounts of missing values [33]. Secondly, commercial-grade sensors commonly used in BMS often lack guaranteed calibration, leading to unknown measurement errors [70]. The placement of sensors may further affect data accuracy, limiting the reliability of data collection [71]. Moreover, only some case studies include labeled fault data, where labels are either generated through fault emulation, similar to those experimental studies, or derived from expert analysis of historical data through a detailed review of the entire measurement period. These challenges in real-world buildings can easily compromise the performance of data-sensitive statistical and machine learning models, highlighting the application potential of DBN with robustness to uncertain measurement and flexibility in modeling approaches. Li et al. [27] determined the prior DBN structure for an industrial building case based on expert knowledge and collected fault data to optimize the DBN using generic algorithms. Taal and Itard [22,46] proposed DBNs for a thermal energy plant and demand-controlled ventilation in a university building case and they examined the diagnosis results based on expert analysis. Gao et al. [68] found DBNs can be tolerant to missing data and still able to correctly identify that heat pumps are not running correctly. Furthermore, compared to case studies, another main practical challenge in implementation studies is real-time data processing. Taal and Itard [23] found that energy performance symptoms, such as coefficient of performance (COP), would be affected by the different detection time spans. Therefore, the input data batch size should be carefully considered in real-time FDD implementation.

While many studies have investigated advanced statistical and machine learning models in simulation and experimental studies, implementation studies play a crucial role in bridging the existing disjunction between academia and the building service industry. Notably, a review by Heimar et al. [11], covering the period from 1980 to 2022, revealed that only 4 % of the papers in the existing literature specifically focused on FDD implementation. These studies highlight critical shortcomings, such as the practical challenges encountered during real-world deployment, which are often overlooked in other study types. Consequently, there is a need for further investigation and development of FDD in building energy systems in real-world implementation scenarios.

3. Methodology

This section will introduce the theoretical fundamentals of DBN, the 4S3F reference architecture, and Kafka-based real-time monitoring framework for HVAC systems.

3.1. Diagnostic Bayesian network

DBNs are probabilistic graphical models that use directed acyclic graphs to represent random events (variables) and their conditional dependencies. DBNs are based on Bayes' theorem [72]. In Bayes theorem, a conditional probability indicates the likelihood of one event occurring given the occurrence of another event. In the context of FDD in building energy systems, $F = \{F_1, F_2, \ldots, F_n\}$ represent a set of possible faults and $S = \{S_1, S_2, \ldots, S_m\}$ represent a set of possible symptom states. If a fault F_i happens when a symptom S is observed or assumed to have occurred, the probability of the fault F_i under the symptom S can be written as follows.

$$P(F_i|S) = \frac{P(F_iS)}{P(S)} = \frac{P(S|F_i)P(F_i)}{P(S)} \tag{1}$$

where $P(F_i|S)$ is the posterior probability of the fault F_i given symptom S; $P(F_iS)$ is the joint probability; $P(S|F_i)$ is the conditional probability of observing symptom S given that fault F_i has occurred; $P(F_i)$ is the prior probability of the fault F_i; $P(S)$ is the marginal probability of observing the symptom S, which can be expressed as follows.

$$P(S) = \sum_{i=1}^{n} P(S|F_i)P(F_i) \tag{2}$$

3.2. 4S3F reference architecture

To systematically and effectively construct DBN for FDD in building energy systems, the 4S3F reference architecture has been

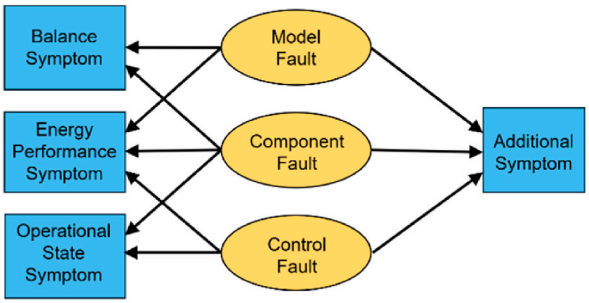

Fig. 1. The illustration of the 4S3F framework.

proposed and applied in Refs. [18,23,24], as illustrated in Fig. 1. The 4S3F architecture, which consists of two stages, closely aligns with HVAC diagrams and the manners in which HVAC systems and their associated control systems are designed [17].

In the first stage, four generic types of symptoms can be detected, which normally are predefined by expert knowledge. Balance Symptoms are detected when balance deviations in energy, mass or pressure balance for systems occur. Energy Performance Symptoms emerge when deviations in energy performance metrics arise, such as COP or energy usage. Operation State Symptoms are detected when the operational states deviate from their expected states arise, such as temperature, flow rate, pressure, and on-off states of components. Additional Symptoms are based on supplementary information, which may include maintenance or inspection records, or fault alerts included in a component by the producer.

In the second stage, three possible faults can be diagnosed through DBNs. Component Faults refer to HVAC components and systems which do not function properly, such as incorrect installation, too low or too high design capacities, fouling, degradation of due to ageing or failure. Sensors are considered as components. These faults are also referred to as “hard faults” [73]. Control Faults include incorrect set points for controllers, timers, on-off control of components, and software faults. For example, this may involve incorrect control of supply temperatures or the on-off sequence of boilers. Model Faults are related to inaccuracies in the quantitative models used to estimate missing or virtual measurements [74]. The control and model faults are also referred to as “soft faults” [73].

3.3. Kafka-based HVAC FDD framework

This study introduces a Kafka-based HVAC FDD framework, as shown in Fig. 2, which is used for real-time data collection and monitoring. The framework is developed using open-source tools, offering scalability, flexibility, and the ability to handle large volumes of data efficiently. It employs Apache software solutions for data acquisition, processing, storage, and visualization. By integrating a suite of advanced tools, the framework ensures robust and efficient FDD for building energy systems, with an emphasis on enabling real-time performance. The following sections provide a detailed overview of the framework’s core software and functionalities.

Apache Kafka [75] is a real-time data stream queuing system designed to publish, store, process, and subscribe to streams of records seamlessly. Its core functionality is to capture and process data in real time from various sources, such as databases and sensors, delivering a continuous stream of events, also referred to as messages. The architecture of Kafka revolves around three key components: producers, consumers, and brokers. Producers are responsible for publishing the events into Kafka. Consumers, on the other hand, subscribe to the events and read them from Kafka. Brokers play a crucial role as mediators between producers and consumers. They efficiently manage and group the events into topics, which are essentially named streams of data. Apache ZooKeeper [76] is employed as a centralized service to maintain configuration information and naming, provide distributed synchronization, and manage group services. InfluxDB [77], an open-source NoSQL time-series database, has been selected for storing timestamped data due to its high performance and reliability. It supports an SQL-like query language, InfluxQL, which allows for querying data from measurements (equivalent to tables in relational databases). Its capabilities make it a reliable storage solution for handling the large volumes of data generated in building systems.

The framework begins with data collection, which involves gathering indoor air quality data, energy consumption data, and control signal records. The collected data is transmitted to a central server, where the Kafka source connector monitors a specified path and forwards the data to Kafka brokers for further processing. Once ingested by Kafka, the data undergoes a series of processing steps before being stored in the main database, InfluxDB. To initiate the FDD process, data is retrieved from InfluxDB and subjected to

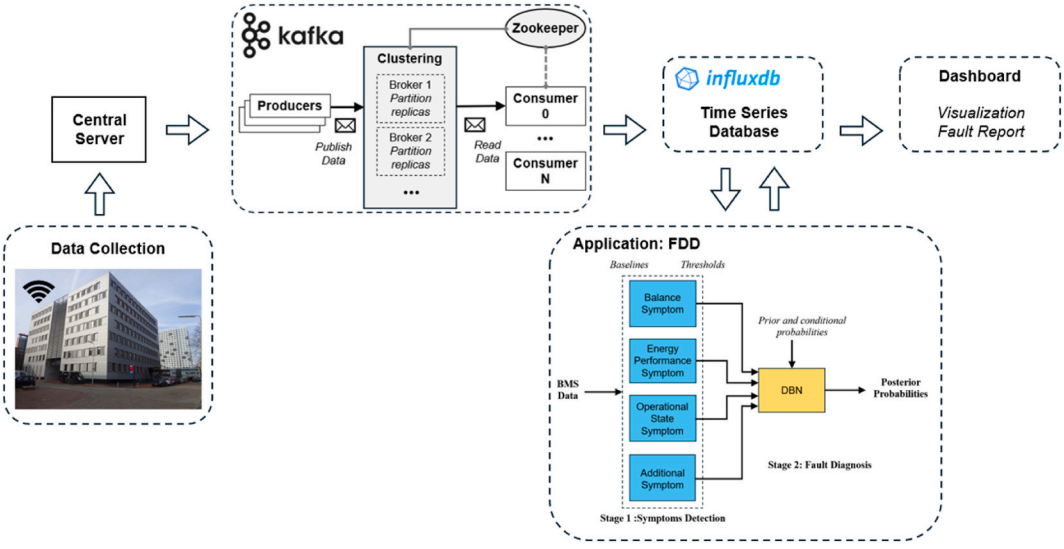

Fig. 2. Kafka-based FDD framework in buildings.

extraction and preprocessing steps. The prepared data is then processed by DBNs, which facilitates symptom detection and fault diagnosis. To monitor the performance of buildings, the posterior probabilities of faults and diagnosis results are stored in the database. Finally, the dashboard can visualize the building operational data and provide fault reports.

Specifically, to support the implementation of the proposed Kafka-based framework, a set of open-source packages was employed in this study. The real-time data streaming and queuing were handled using confluent-kafka (version 2.4.0), while time-series data storage and querying were managed through influxdb-client (version 1.43.0). For numerical processing, pandas (version 2.2.1) and numpy (version 1.26.4) were used, respectively. The DBNs were implemented using the pgmpy library (version 0.1.25). These tools enabled the development of a scalable, efficient, and interpretable FDD system tailored for real-world HVAC applications.

4. Case study

This section provides an overview of the case building, covering the HVAC system P&ID, sensor configuration, and control strategies. It also introduces the proposed DBN construction, including problem formulation, structure modeling, parameter modeling, fault isolation and evaluation.

4.1. Case description

The case study involves an AHU installed in a seven-floor office building on the campus of TU Delft, the Netherlands. The building was built in 2002 with a total area of 10,767 m^2. This AHU is equipped with filtering, heat recovery, and both heating and cooling capabilities, with airflow up to 28,700 m^3/h. Heating is supplied by two gas-powered boilers, while cooling is provided by a chiller, both located in the building's basement. The simplified piping and instrumentation diagram (P&ID) of the AHU is shown in Fig. 3. All the monitoring variables in the BMS are listed in Table 2, including temperature, static pressure, pressure difference, setpoints, control signals, and component alerts.

Fig. 4 presents the simplified operational strategies of the AHU from the system document, which is originally in Dutch. The AHU heats or cools the air depending on the supply air temperature relative to its setpoint. The x-axis represents the temperature, ranging from cold to warm. The y-axis represents the control signal, ranging from 0 % (fully closed) to 100 % (fully open). Unlike AHUs with mixing air chambers in the other studies [16,19,20,27,40,41], the AHU is equipped with a HRW, which can be used to exchange heat or cold between supply and return airflows to save energy. The technical specification states 49 % of the supply efficiency and 81 % of the exhaust efficiency of the HRW. If the supply air temperature falls below the setpoint in the heating season, the HRW is first activated. If the desired temperature cannot be reached by the HRW alone, the boiler starts to work, and the heating coil valve (HCV) opens to further increase the temperature. When the supply air temperature exceeds the setpoint in the cooling season, the chiller starts to work, and the cooling coil valve (CCV) opens further to reduce the temperature to the desired level. The valves regulate the flow of warm or cold water through the coils, which in turn transfer heat or cooling to the air being supplied. During winter, the CCV remains inactive, and similarly, the HCV is not used in summer.

Fig. 5 illustrates the rule-based strategies for adjusting the supply air temperature setpoint based on the outdoor temperature.

Ventilation of the AHU is provided by a set of fans located at the end of the supply and return ducts, with pressure in the ducts monitored by pressure sensors. The AHU adjusts fan speed to ensure the measured pressure matches the supply and return pressure setpoints, which are consistently set to 185 Pa and 200 Pa, respectively, as specified by the BMS. Airflow into and out of the AHU is regulated by one supply damper and two return dampers. Dampers, which are valves or plates that control airflow, in this case study are only operated as fully open or close. The supply damper automatically opens when the supply fan is activated by the AHU, while

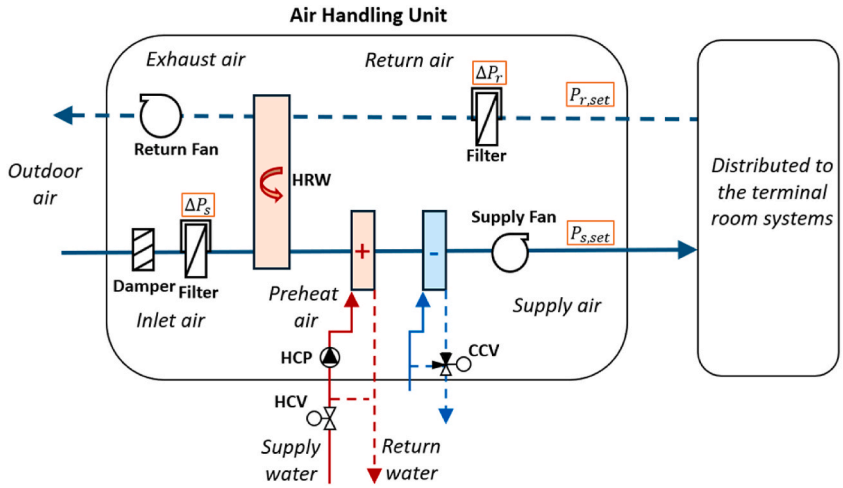

Fig. 3. The simplified P&ID of the AHU.

Table 2
Variables in BMS.

Variable	Description	Variable	Description
T_o	Outdoor air temperature	$P_{r,set}$	Return air pressure setpoint
T_i	Inlet air temperature	U_{hcv}	HCV control signal
T_p	Preheated air temperature	U_{hrw}	HRW control signal
T_s	Supply air temperature	$U_{s,fan}$	Supply fan control signal
T_r	Return air temperature	$U_{r,fan}$	Return fan control signal
T_e	Exhaust air temperature	$A_{s,fan}$	Supply fan alert
P_s	Supply air pressure	$A_{r,fan}$	Return fan alert
P_r	Return air pressure	$A_{s,filter}$	Supply filter alert
ΔP_s	Pressure difference between supply filter	$A_{r,filter}$	Return filter alert
ΔP_r	Pressure difference between return filter	A_{hrw}	HRW alert
T_{set}	Supply air temperature setpoint	A_{hcp}	HCP alert
$P_{s,set}$	Supply air pressure setpoint		

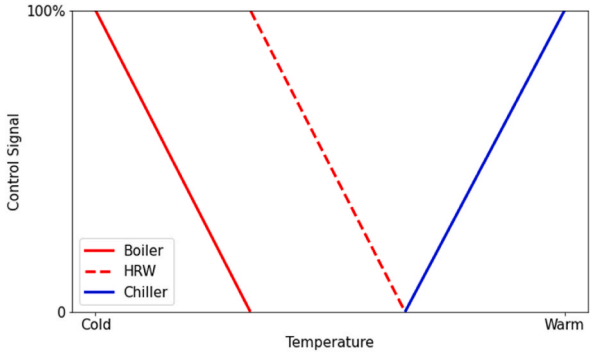

Fig. 4. Simplified operational strategies of the AHU from the design documents.

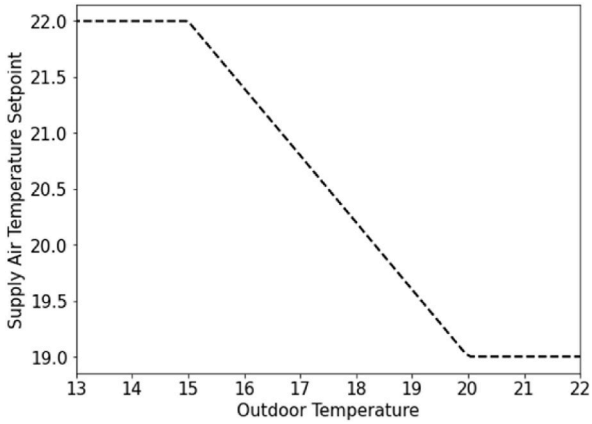

Fig. 5. The supply air temperature setpoint of the AHU from the design documents.

the two return dampers, located on the east and west sides of the building, are controlled by the BMS and open during working hours. Additionally, the AHU includes two air filters, one in the supply duct and one in the return duct, both positioned before the HRW. These filters help maintain cleanliness within the AHU and purify the air being supplied. Pressure difference sensors monitor the condition of the filters, indicating when replacement is needed, as the pressure difference increases with accumulated dust. Additionally, the BMS includes three seasonal modes: winter, summer, and in-between seasons. The operation of the coils, boilers, and chiller is adjusted depending on the active season, with these components either blocked or unblocked as needed. The system also integrates online weather data and has functionality for generating alerts based on sensor readings.

4.2. DBN construction

In this study, a DBN is proposed for the FDD task in the AHU of the case building. The DBN is constructed following the four-step modeling procedure outlined in Ref. [17], including problem formulation, structure modeling, parameter modeling, and fault isolation.

4.2.1. Problem formulation

The first step, problem formulation, involves understanding the components, capacities, sensors, and control in the system, identifying potential faults, and defining the symptoms of the FDD process.

In this study, the common faults, along with their associated symptoms, are determined based on the literature [5,19,21,78]. The faults primarily focus on component and control-related issues, with a total of 26 faults. Some similar faults, such as supply fan (Fan_s) stuck and return fan (Fan_r) stuck, are grouped under a single fault number for simplification and clarity. Then, there are 35 symptoms identified, most of which are related to the operational states of the system as defined in the design documents. Due to the absence of airflow and water flow sensors, accurately calculating energy performance becomes challenging. However, two symptoms are used to approximately estimate the energy efficiency of the heating coil and the HRW. Alerts in the system are classified as additional symptoms. Additionally, the thresholds ε determine the sensitivity of symptoms and have a significant effect in determining when

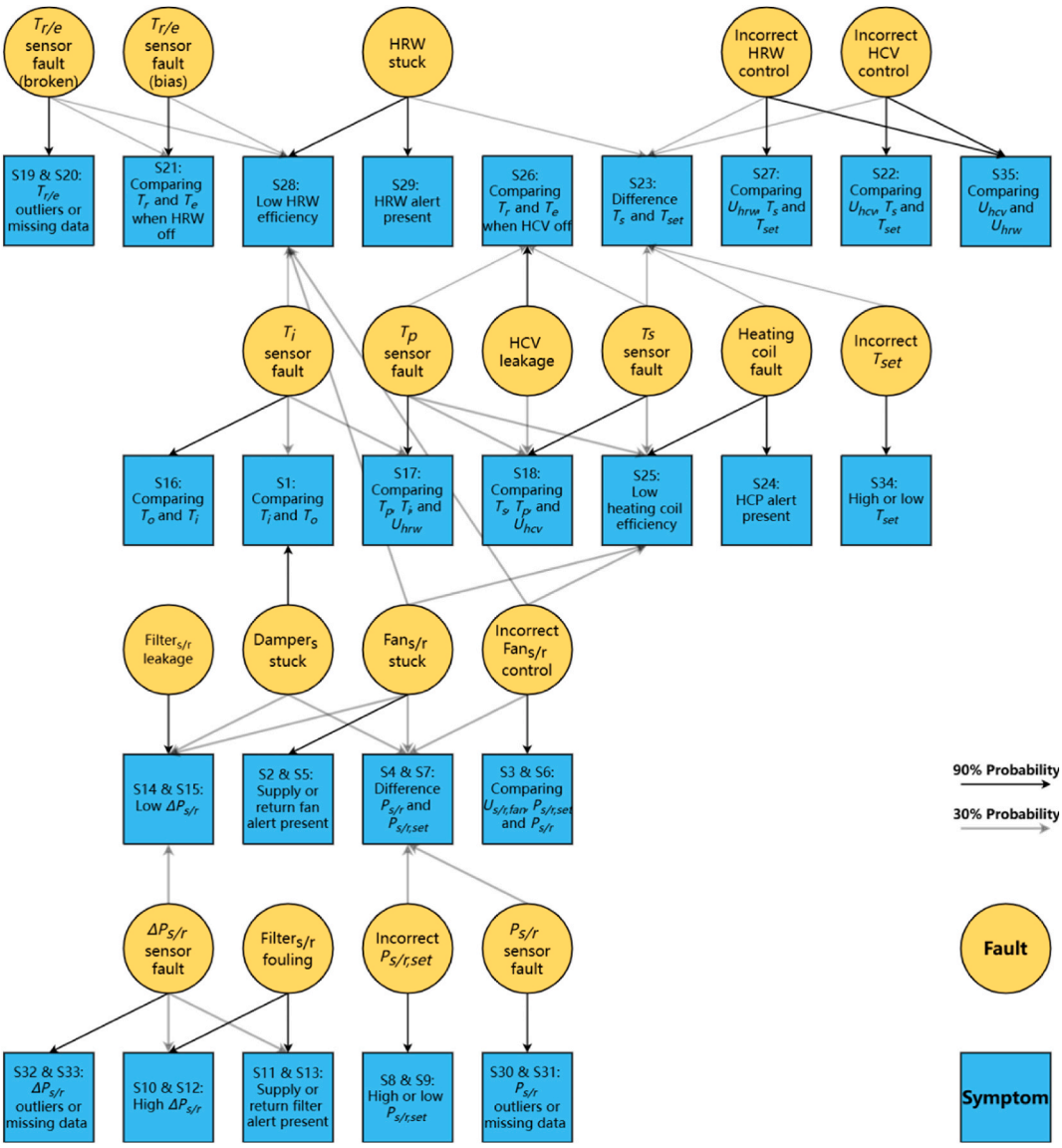

Fig. 6. The proposed DBN for the AHU in the case building.

symptoms are detected. For example, ε1 is the temperature deviation between Ti and To, which are expected to be equal under normal conditions. In this study, ε1 is set to 2 °C. If the deviation exceeds this threshold, it is considered a symptom indicating abnormal behavior. When the thresholds are set too high, only severe deviations will be detected as symptoms, increasing the risk of false negatives. Conversely, when the thresholds are too low, normal fluctuations in system operation may trigger symptom detection, leading to false positives. The specific ε values chosen for symptoms are defined heuristically by design documents, expert knowledge and experience. A complete list and description of all faults, symptoms and thresholds can be found in the Appendix A1, A2, and A3 respectively.

In the proposed DBN, both symptoms and faults are defined to have only two possible states: *Present* or *Absent*. This binary representation simplifies the construction of the DBN. Despite this simplification, it still provides building managers with sufficient fault information in practice.

4.2.2. Structure modeling

Then, structure modeling involves constructing the structure of the BN model, reflecting the dependencies between the fault nodes and symptom nodes. The proposed DBN is based on expert knowledge, shown in Fig. 6.

In Fig. 6, some faults and symptoms that appear on components or sensors of both the supply and return sides of the AHU are combined and denoted with a subscript "s/r". The structure of connections to symptom nodes differs depending on whether the symptom node is also combined. If the symptom node is combined, the supply-side fault is linked to the supply-side symptom, and the return-side fault is connected to the return-side symptom. For instance, the top-left "$T_{r/e}$ fault (broken)" fault node represents the $T_{r/e}$ fault connected to symptom S19 and the T_e fault connected to symptom S20. In cases where a symptom node represents a single symptom, both supply and return faults are connected to it. For example, the connection from the "$T_{r/e}$ fault" to symptom S21, where both the T_r and T_e faults are linked to symptom S21. The "Damper_s stuck" fault is connected only to supply-side symptoms S14 and S4, as these symptoms pertain specifically to the supply side of the AHU.

4.2.3. Parameter modeling

This step involves specifying the parameters of the DBNs, including assigning prior probabilities and conditional probabilities.

Prior probabilities refer to the frequency of fault occurrence in building energy systems. However, there is a lack of understanding of how often each fault occurs in AHUs with HRW. Yet, the possibility of faults occurring is still considered low. In this study, for component faults, the initial prior probabilities are assigned as 0.02 for fault *Present* state and 0.98 as fault *Absent* state. For control faults, initial prior probabilities are assigned as 0.05 for fault *Present* state and 0.95 as fault *Absent* state. Therefore, it is expected that component faults have a 2 % probability of being *Present*, while control faults have a 5 % probability, independent of any other faults or symptoms.

Due to simplified binary representation of faults and symptoms, it requires only one parameter for each conditional probability between a fault and its associated symptom. The conditional probabilities of DBN have been grouped into two types: strong and weak relationships. As depicted in Fig. 6, black edges indicate strong conditional probabilities of 90 %, while grey edges represent weak conditional probabilities of 30 %. Theoretically, distinct conditional probabilities can be defined for every edge in the DBN, but this becomes cumbersome in practice. Furthermore, Taal et al. [23] have shown that the chosen absolute conditional probability values are less important than the relative values.

For each component fault, the conditional probability of the related alert symptom was set to strong. If a fault had no related alert, the most likely symptom was considered strong. This approach was made possible because symptoms were formulated to correspond to the chosen faults. The HRW and heating coil efficiency symptoms were also considered strong conditional probabilities for the HRW and heating coil failure faults. Symptom S23 can be caused by multiple control, component or sensor faults, also same with symptoms S4 and S7, which are detected when the measured pressure is different from the setpoint. Therefore, they have no strong conditional probability edges, as the possible faults are too many to be certain which fault likely caused it. The entire conditional probability table (CPT) for each symptom node is constructed with the leaky-or model based on the conditional probabilities. The CPT of a symptom node contains probability for each combination of fault states that are connected to the node.

4.2.4. Fault isolation and evaluation

The step involves calculating the fault posterior probabilities based on observed symptoms and isolating the faults according to predefined rules. In this study, the diagnosis using the proposed DBN is performed on both historical and experimental data.

Exact Bayesian inference is the most common algorithm to calculate the posterior probabilities of faults in building energy systems. In this study, we also use it to perform a backward inference to find the most probable fault given the observed symptoms, as shown in Equation (2). In this study, a fault is considered to be diagnosed if its posterior probability is at least 60 %. Unlike single fault diagnosis in Refs. [19,20,40], the proposed DBN supports multiple fault diagnosis at the same time.

For the historical data analysis, records from 2022 to 2023 were selected, focusing exclusively on working hours. The dataset spans a total of 506 working days, with measurements recorded at 10-min intervals, resulting in 36,433 samples. To minimize false positives due to unstable measurements in practice, the detection of a symptom sample requires at least two consecutive samples to exhibit the *Present* state. To confirm the daily detection of a symptom on a given day, the symptom must appear in at least three samples within that day. Subsequently, daily fault diagnosis is performed using the proposed DBN, which leverages these daily symptom detections to calculate the posterior probabilities of each fault. Some metrics are defined in the historical analysis, including the *sample-level symptom detection rate, day-level symptom detection rate,* and *day-level fault diagnosis rate*. The sample-level symptom detection rate refers to the proportion of detected samples to the total number of samples, while the day-level symptom detection rate refers to the

proportion of days with detected symptoms to the total number of analyzed days. The day-level fault diagnosis rate refers to the proportion of days with diagnosed faults to the total number of analyzed days.

For the experimental data analysis, nine experiments are conducted to simulate four types of control faults. The details of the fault experiments are presented in Table 3. Similar to the historical data analysis, symptom detection across different time periods requires a minimum of $p/6$ occurrences of a detected symptom within the period to confirm its presence, where p is the number of samples in the period. The detected symptoms are then used for fault diagnosis during this period.

5. Results

This section presents data analysis and diagnosis results from the proposed DBN, using both historical and experimental data.

5.1. Statistical analysis of historical data

The statistical analysis of historical data reveals some interesting insights. Fig. 7(a) presents the distribution of temperature-related variables from 2022 to 2023, including temperature sensors and supply air temperature setpoints. First, the values from T_o and T_i sensors show similar distributions. However, the T_i sensor values, with an average of 14.4 °C, are slightly higher than the T_o sensor values, which have an average of 13.7 °C. The T_o data comes from an online weather source integrated into the BMS, while T_i sensor data comes from BMS measurement. Consequently, the difference could be due to a bias in one of the temperature readings or differences in the measurement locations. Additionally, T_{set} can sometimes be set lower than 19 °C, even as low as 10 °C, which is inconsistent with the description in the design documents as shown in Fig. 5. Fig. 7(b) presents further details about the T_o and T_{set}. According to the design documents, the T_{set} is set based on the T_o, which is represented by the nominal setpoint curve in the figure. But the actual setpoints are consistently much lower than the curve. This suggests that the system might be operating outside the parameters outlined in the design documents and these deviations could be the result of system misconfigurations, sensor calibration issues, or a deliberate adjustment based on user preferences.

Fig. 8 shows the distribution of the pressure-related variables, including static pressure sensors, pressure difference sensors, and pressure setpoints. As expected from the design documents, the median values of the setpoints $P_{s,set}$ and $P_{r,set}$ are 185 Pa and 200 Pa, respectively, and the actual pressure values (P_s and P_r) align well with their setpoints, except for a few outliers.

Fig. 9 shows the distribution of control-related variables. First, the distributions of the CCV and HCV control signals exhibit a broad range, reflecting the varying heating and cooling demands influenced by outdoor weather conditions. This is consistent with the Dutch climate, where heating is required more frequently than cooling. Consequently, the cooling coil is utilized on fewer days than the heating coil, resulting in a median value of 0 %. Next, the median values of the fan control signals align with the required control settings to maintain the pressure setpoints. The interquartile range is relatively narrow, as expected, given that the pressure setpoints are fixed and do not fluctuate. Third, the control signal for the HRW spans from 0 % to 100 %, as it operates with binary control—either off (0 %) or on (100 %). This binary operation can complicate the maintenance of a stable supply temperature, as the HRW might need to be frequently switched on and off to achieve the desired setpoint, rather than maintaining a constant capacity like the valves. The median value for the HRW control is 100 %, indicating that the HRW was typically in the 'on' state.

5.2. Diagnosis on historical data

Fig. 10 presents the results of symptom detection in historical data. Eleven symptoms were not detected on any day, while another eleven symptoms were detected on over 10 % of the days. Among these detected symptoms, symptoms S19 and S16 appeared nearly every day, along with symptoms S25, S23, S22, S34, S1, S17, S27, S35, and S18. These detected symptoms reveal several issues in real-building scenarios, including sensor performance and control operations.

Sensor-related issues are evident in the frequent detection of symptom S19 is due to the return air temperature sensor data being only available in 30-min intervals and containing missing values, reflecting the challenges of varying sensor granularity. The detection of symptoms S1 and S16 reveals the inconsistencies between the T_i sensor and the T_o sensor as the discrepancy mentioned in Section 5.1. Similarly, symptoms S17 and S18 highlight further inconsistencies between sensor values. Symptom S17 points to discrepancies between the T_i sensor and the T_p sensor when the HRW is off, while symptom S18 reflects inconsistencies between the T_p sensor and the

Table 3
The details of the fault experiments.

Case	Simulated Fault	Experiment Description	Time	Date
1	Incorrect Fan_s control	Fan_s control signal was set to 30 %	08:30–11:00	2024.3.23
2	Incorrect Fan_s control	Fan_s control signal was set to 70 %	11:30–14:00	2024.3.23
3	Incorrect $P_{s,\ set}$	$P_{s,\ set}$ was set to 235 Pa	11:10–13:50	2024.3.24
4	Incorrect $P_{s,\ set}$	$P_{s,\ set}$ was set to 135 Pa	14:00–17:00	2024.3.24
5	Incorrect HCV control	HCV control signal was set to 0 %	9:30–11:20	2024.3.29
6	Incorrect HCV control	HCV control signal was set to 30 %	11:30–14:00	2024.3.29
7	Incorrect HCV control	HCV control signal was set to 100 %	14:05–17:00	2024.3.29
8	Incorrect T_{set}	T_{set} was set to 23 °C	11:30–14:30	2024.3.30
9	Incorrect T_{set}	T_{set} was set to 17 °C	14:35–17:59	2024.3.30

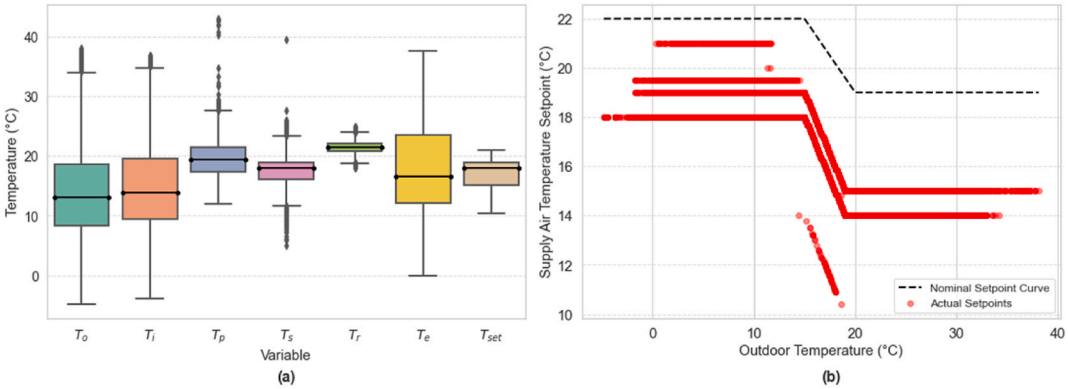

Fig. 7. The distribution of the temperature-related variables in 2022–2023: (a) the boxplot of the temperature-related variables; (b) comparison between the supply air temperature setpoints and the outdoor temperature.

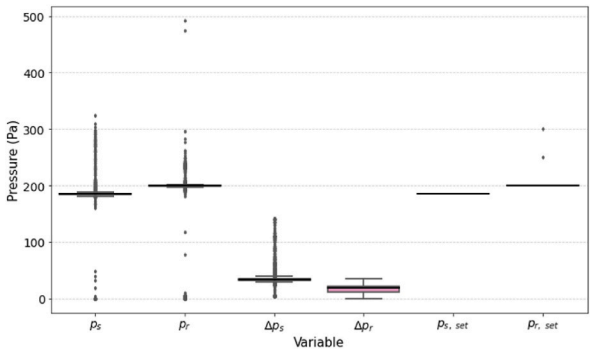

Fig. 8. The boxplot of the pressure-related variables.

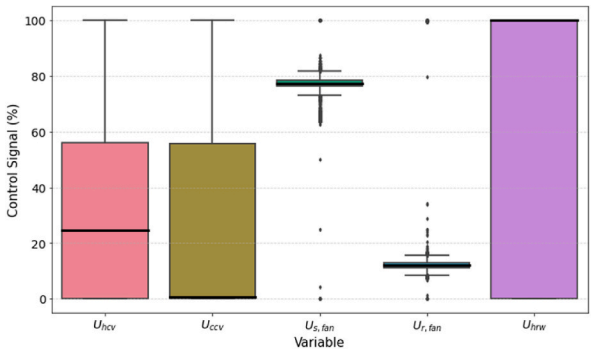

Fig. 9. The boxplot of the control-related variables.

T_s when the HCV is off. Both symptoms suggest potential sensor bias or sensor placement issues. Also, the detection of symptom S25 indicates the T_s is lower than expected. One possible cause for symptom S25 could be sensor bias in either the T_p or T_s measurements.

Control-related issues are reflected in the presence of symptom S23, which indicates that the T_s often deviates by more than 1 °C from its setpoint, suggesting potential faults with the HCV and HRW controls, similar to the presence of symptom S22. Meanwhile, the presence of symptom S34 indicates that the T_{set} was not between 19 °C and 22 °C, reflecting inconsistencies with the control strategies specified in the design documents, as mentioned in Section 5.1. Similarly, symptom S35 is formulated according to design specifications requiring the HRW to operate at 100 % when the HCV starts working. The frequent presence of S35 also shows the inconsistencies between design and actual operations. Also, another potential cause of symptom S25 could be inaccuracies in the HCV control signal, leading to an inability to consistently deliver the required heat.

Additionally, if the day-level symptom detection rate is higher than the sample-level symptom detection rate, this indicates that the symptom is present on most days but occurs only a few times per day. Conversely, if the sample-level symptom detection rate is higher

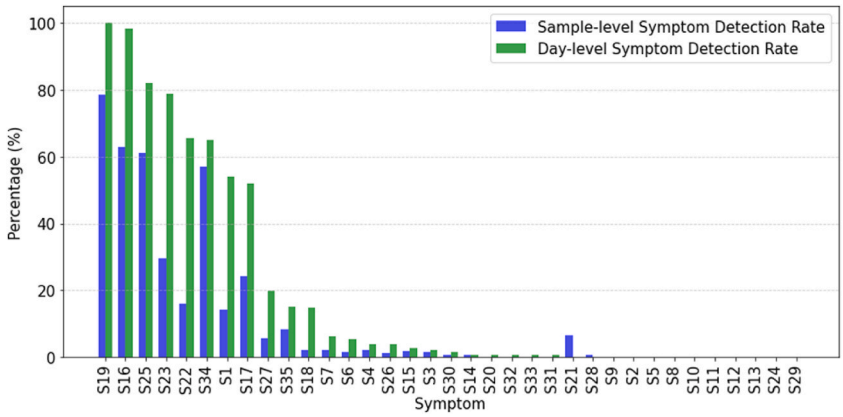

Fig. 10. Symptoms detection rate in historical data from 2022 to 2023.

than the day-level symptom detection rate, the symptom tends to be detected on fewer days throughout the year, possibly correlating with seasonal patterns. Interestingly, the ratio between day and sample level symptom detection rates varied significantly across symptoms. For example, symptoms S23 and S25 were detected on a similar number of days, although symptom S25 had nearly twice as many detected samples as symptom S23. Most symptoms showed a higher day-level detection rate than the sample detection rate, with S21 being an exception. This suggests that S21 tended to appear more frequently in short bursts over fewer days.

Fig. 11 presents the results of fault diagnosis in historical data. Six faults were diagnosed on more than 10 % of the days. The most frequently diagnosed fault was the "T_r Sensor Fault", which was diagnosed on all days in the dataset. This is expected due to the missing data for the return air temperature sensor, as indicated by symptom S19. The "T_i Sensor Fault" was also frequently diagnosed, occurring on 97 % of the days, aligning with the frequent detection of symptoms S16 and S1. Similar to the "T_p Sensor Fault" with the related symptoms S26, S18, and S25. The "Incorrect $T_{s,set}$" was detected on 64 % of the days, due to the strong link to symptoms S34 and S23. Control faults such as "Incorrect HCV Control" and "Incorrect HRW Fault" were detected on 43 % and 11 % of the days, respectively, with related symptoms S23, S27, S22, and S35 detected beforehand. The remaining faults were diagnosed infrequently, which aligns with the related symptoms that were also detected infrequently.

Fig. 11 also presents the average posterior probabilities of each fault and the comparison between average posterior probabilities and day-level fault diagnosis rates provides some insights. For the most frequently diagnosed six faults, the values of the average posterior probabilities closely align with the percentage of days they were detected. It is because, on days when these faults were diagnosed, their posterior probabilities were nearly 100 %. Conversely, on days when they were not diagnosed, the probabilities were generally close to 0 %. For "T_s Sensor Fault", "HC Fault", and "Fan_s Stuck", the average posterior probabilities are relatively high despite the percentage of diagnosed days ranging only from 2 % to 5 %. This suggests that the calculated daily posterior probabilities for these faults were frequently above 0 %, yet insufficient to surpass the posterior probability threshold of 60 % for fault diagnosis, thereby preventing their diagnosis on many days.

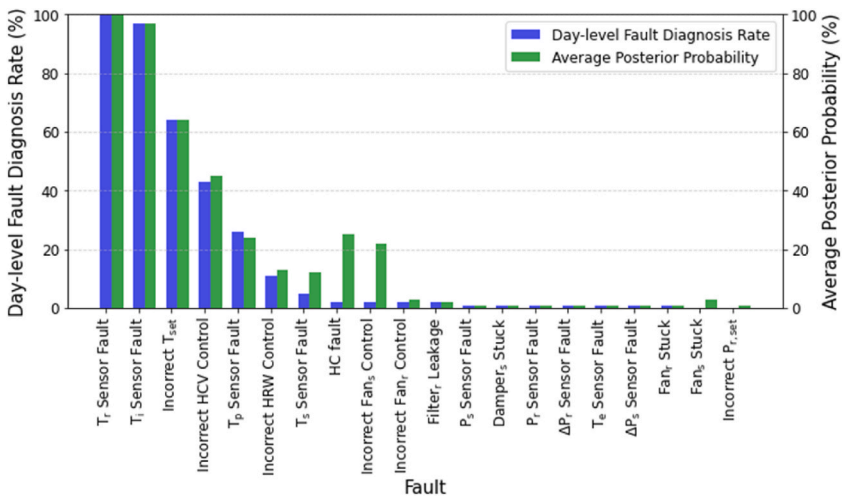

Fig. 11. Fault diagnosed in historical data from 2022 to 2023.

5.3. Diagnosis on experimental data

To further evaluate the capabilities of the DBN, nine fault experiments were conducted. Table 4 provides a summary of the diagnostic results from the experimental data, presenting the top three faults ranked by their posterior probabilities. Faults in bold indicate the correct diagnosis. The results demonstrate that DBN effectively identifies eight out of nine simulated faults. However, some unexpected faults are also diagnosed. A detailed analysis of these diagnoses is provided below.

In Case 1, the fault "Incorrect Fan Control" is accurately diagnosed with a posterior probability of 100 %. This is because the P_s decreases when the supply fan is stuck at a low speed, resulting in the presence of the relevant symptoms S3 and S4. However, two additional faults, "T_i Sensor Fault" and "Incorrect HCV Control", are also observed both with posterior probabilities of 100 %. First, the diagnosis of "T_i Sensor Fault" is based on the presence of the highly relevant symptom S16. As previously observed in the historical data analysis, the value of the T_i sensor appears abnormal, suggesting that the sensor may have been installed at an inappropriate location. Second, the diagnosis of "Incorrect HCV Control" can be attributed to unexpected system behavior. At lower fan speeds, the HCV control signal becomes unstable, causing fluctuations in the supply air temperature. This situation results in the presence of relevant symptoms S22 and S23, which contribute to the diagnosis. In Case 2, the fault "Incorrect Fan Control" is also accurately diagnosed with a posterior probability of 100 %. When the supply fan is stuck at a higher speed, the relevant symptoms S3 and S4 get detected. However, similar to Case 1, the presence of symptoms S1 and S16 leads to the diagnosis of an additional fault, "T_i Sensor Fault". Additionally, the unstable HCV control causes the detection of symptom S23, resulting in the false-positive diagnosis of the fault "Incorrect $T_{set.}$".

In Cases 3 and 4, the fault "Incorrect $P_{s,\ set}$" is easily diagnosed by the presence of the highly relevant symptom S8.

In Case 5, the fault "Incorrect HCV Control" is accurately diagnosed with a posterior probability of 100 %. Due to the HCV control signal being stuck at 0 %, the heating coil is unable to provide sufficient heat, preventing the T_s from reaching its setpoint. This results in the presence of the relevant symptoms S22 and S23. However, an additional fault, "T_s Sensor Fault", is also diagnosed due to the presence of symptom S18. This is unusual because, when HCV is fully closed, T_s is even lower than T_p. A possible explanation is that the fault in the T_s sensor may indeed exist, or the sensor might be improperly installed. In Case 6, the fault "Incorrect HCV Control" is also accurately diagnosed with a posterior probability of 100 %, based on the symptoms S22 and S23. But there is an additional fault, "Heating Coil Fault", with a posterior probability of 52.7 %. It is due to the presence of the relevant symptom S25, which is triggered by the abnormal values of T_s as mentioned above. In Case 7, the simulated fault "Incorrect HCV Control" is misdiagnosed to "T_i Sensor Fault" with a posterior probability of 100 % and "Heating Coil Fault" with a posterior probability of 80.6 %. "T_i Sensor Fault" could be a potential system fault as previously analyzed. The diagnosis of "Heating Coil Fault" arises because of the presence of symptoms S23 and S25: during the experiment, T_s did not increase as expected when the HCV control signal was set to 100 %, likely due to the boiler being unexpectedly shut off.

In Case 8, the fault "Incorrect T_{set}" is accurately diagnosed with a posterior probability of 100 %, directly attributed to the presence of symptom S34.

But in Case 9, except for the correct diagnosis, two additional faults, "T_i Sensor Fault" and "Incorrect HCV Control", are also diagnosed. "T_i Sensor Fault" is consistent with previous cases, likely caused by the T_i sensor's improper installation, which triggers symptom S16. The diagnosis of "Incorrect HCV Control" is because when T_{set} is set too low, the HCV attempts to adjust but behaves unstably, leading to unexpected system behavior and activating the symptoms S22 and S23.

6. Insights, limitations, and future directions

In this study, DBNs are implemented to support FDD in the heat recovery ventilation system. The DBN approach offers several unique advantages. First, it provides high interpretability by aligning with HVAC engineering logic and causal relationships, which facilitates understanding and trust among practitioners. Second, DBNs are robust to missing or noisy sensor data. Third, DBNs can support simultaneous multi-fault diagnosis, making them well-suited to the inherent complexity and multi-fault nature of real-world scenarios, where purely data-driven models may fail or need to re-train. Furthermore, the integration with Kafka-based framework also demonstrates their feasibility for real-time implementation. The DBN in this study is constructed entirely based on expert knowledge, without requiring any training data. In summary, compared to data-driven or simple rule-based methods, the DBN approach provides a strong balance of diagnostic accuracy, transparency, and modeling flexibility.

By combining detailed diagnosis analysis based on both historical and experimental data, the study offers valuable insights into FDD for the AHU system equipped with HRW. The main findings of this study are summarized as follows.

- First, the statistical analysis of historical data reveals significant discrepancies between the design documents and the actual operation of the HVAC system. These include potential biases in sensor measurements and consistently lower-than-nominal temperature setpoints, indicating poor commissioning practices and possible occupant interventions that may have led to deliberate adjustments of setpoints, which are often observed in real-world building scenarios.
- Second, fault diagnosis on historical data further emphasizes these discrepancies and uncovers inherent sensor faults, such as installation issues, missing or inconsistent data. It also identifies distinct symptoms and fault patterns that some symptoms persist on most days but occur only occasionally throughout the day, while others appear in short bursts over fewer days, potentially correlating with seasonal effects.
- Third, in the diagnosis on experimental data, the proposed DBN demonstrates its effectiveness by successfully identifying eight out of nine simulated faults, confirming its capability as an FDD tool. However, the DBN also diagnoses additional, unexpected faults.

Table 4
Diagnosis results on experimental data.

Case	Rank of Posterior Probability					
	No.1	Posterior probability	No.2	Posterior probability	No.3	Posterior probability
1	**Incorrect Fans Control**	100 %	T_i sensor Fault	100 %	Incorrect HCV Control	100 %
2	**Incorrect Fans Control**	100 %	T_i Sensor Fault	100 %	Incorrect T_{set}	75.1 %
3	**Incorrect $P_{s,\ set}$**	100 %	Incorrect $P_{r,\ Set}$	0.4 %	Incorrect Fan_r Control	0.3 %
4	**Incorrect $P_{s,\ set}$**	100 %	Incorrect $P_{r,\ Set}$	0.4 %	Incorrect Fan_r Control	0.3 %
5	**Incorrect HCV Control**	100 %	T_s Sensor Fault	94.4 %	HCV Leakage	3.9 %
6	**Incorrect HCV Control**	100 %	Heating Coil Fault	52.7 %	Incorrect Fan_s Control	26.6 %
7	T_i Sensor Fault	100 %	Heating Coil Fault	80.6 %	T_s sensor Fault	18.9 %
8	**Incorrect T_{set}**	100 %	Incorrect $P_{s,\ Set}$	0.4 %	Incorrect $P_{r,\ set}$	0.4 %
9	**Incorrect T_{set}**	100 %	T_i Sensor Fault	100 %	Incorrect HCV Control	100 %

These can be attributed to three factors: (1) false positives arising from the DBN's inability, (2) inherent system faults as mentioned in historical data analysis, or (3) unexpected HVAC system behavior triggered by the simulated faults. Notably, inherent system faults should not be regarded as false positives, as these faults genuinely exist within the building and are common in poorly commissioned real-world conditions. Despite these challenges, the DBN remains effective, whereas purely data-driven methods might fail under such conditions.

Despite its contributions, the study has several limitations. First, the analysis is based on data from a single building in the Netherlands, which may limit the generalizability of the findings to other buildings or HVAC systems with different configurations, operational characteristics, or environmental conditions. Second, the development of the DBN, including its structure, parameters, and thresholds, was based on the authors' domain knowledge and analysis, which is a common practice in other related studies [19,20,40]. But the proposed DBN may not fully account for all potential symptoms or fault behaviors, particularly in real-world scenarios where inherent system faults and unexpected operational dynamics can further complicate system behavior. Furthermore, this approach also poses challenges when applying DBN to other buildings. While the general DBN-based FDD framework is conceptually transferable, its practical application to other buildings involves several system-specific adaptations. The network structure, parameters, and symptom thresholds are typically tailored to the specific HVAC system, sensor configurations, and fault definitions of the target building task. Therefore, significant customization may be required. However, certain parts of the framework are reusable or adaptable across buildings. For example, prior probabilities and conditional dependencies associated with common HVAC components (e.g., fans, dampers, HRWs) may be transferable, especially in buildings with similar control strategies and sensor availability. The Kafka-based data stream framework can also be reused with minimal modification.

Future work could address these limitations and enhance the robustness of DBNs for FDD in real-world building scenarios. First, due to frequent issues with missing sensor values, it is valuable to explore sensor data imputation methods and virtual sensor techniques to mitigate data quality issues. Second, given the frequent occurrence of inherent system faults and the potential for multiple faults to overlap or interact, investigating the effects and patterns of simultaneous faults could offer valuable insights for the construction of DBNs, such as symptom determination, structure and parameter modeling. Furthermore, developing adaptive threshold mechanisms could enhance the flexibility and accuracy of DBN across different systems and operational characteristics. Lastly, in real-world scenarios, experts may have differing opinions on fault frequency and patterns, influenced by their background and experience. To enhance DBN's reliability, it would be beneficial to incorporate insights from multiple experts in determining the prior and conditional probabilities.

7. Conclusions

This study presents the implementation of DBNs in Dutch office building, demonstrating their potential and challenges for FDD in real-world building scenarios. A Kafka-based framework is introduced for implementing FDD in HVAC systems. By integrating detailed diagnostic analysis using both historical and experimental data, the study provides valuable insights into FDD for AHU systems equipped with HRW. Statistical analysis of historical data reveals notable discrepancies between design specifications and actual HVAC operation. Fault diagnosis on historical data further exposes these discrepancies, identifying inherent sensor faults such as installation errors, missing data, and inconsistencies. These insights can inform improvements in building service practices, including refining maintenance protocols and supporting continuous commissioning. The proposed DBN model proves its capability by accurately detecting eight out of nine simulated faults in experimental data, despite some false positive diagnoses. Future work should focus on addressing these limitations to enhance the robustness and reliability of DBNs for FDD in real-world building scenarios. Key areas for improvement include further investigating fault impact, enabling simultaneous fault diagnosis, developing adaptive threshold mechanisms for improved symptom detection and fault diagnosis, and integrating expert knowledge to enhance model ability and decision-making.

CRediT authorship contribution statement

Lars van Koetsveld van Ankeren: Writing – original draft, Methodology, Investigation, Formal analysis. **Chujie Lu:** Writing –

original draft, Visualization, Supervision, Methodology, Investigation, Formal analysis, Data curation, Conceptualization. **Laure Itard:** Writing – review & editing, Supervision, Project administration, Methodology, Funding acquisition, Conceptualization.

Declaration of competing interest

The authors declare that they have no known competing financial interests or personal relationships that could have appeared to influence the work reported in this paper.

Acknowledgements

This study is a part of the Brains4Buildings project, sponsored by the Dutch grant program for Mission-Driven Research, Development, and Innovation (MOOI), which is established by the Dutch Ministry of Economic Affairs and Climate Change and the Ministry of the Interior and Kingdom Relations and executed by RVO Netherlands Enterprise Agency. The authors appreciate the Campus Real Estate & Facility Management at TU Delft for data collection, system and experiment settings. Additionally, the authors sincerely appreciate Dr. Arie Taal for the valuable discussion.

Appendix. The details of the proposed DBN

Table A1
The fault nodes in the proposed DBN

No.	Fault	Description	Fault Type
F1	Fan_s/Fan_r Stuck	The supply or return fan is stuck or fails completely.	Component
F2	$Filter_s$/$Filter_r$ Leakage	Air is leaking when passing the supply or return filter.	
F3	$Filter_s$/$Filter_r$ Fouling	The supply or return filter is filled with dirt or dust.	
F4	Heating Coil Fault	HCV stuck or HCP failure	
F5	HCV Leakage	Heating water leaks through the valve, causing the heating coil to heat the air up even when the HCV is fully closed.	
F6	HRW Stuck	The HRW is stuck or fails completely.	
F7	$Damper_s$ Stuck	The supply damper is stuck.	
F8	P_s/P_r Sensor Ault	The supply or return air pressure sensor exhibit biases, outliers or missing values.	
F9	ΔP_s/ΔP_r Sensor Fault	The pressure difference sensor between supply or return filter exhibit biases, outliers, or missing values.	
F10	T_b/T_p/T_s/T_r/T_e Sensor Fault	The inlet, preheat, supply, return or exhaust air temperature sensor exhibit biases or broken (outliers, or missing values).	
F11	Incorrect T_{set}	The AHU supply air temperature setpoint is higher or lower than the designed setpoint.	Control
F12	Incorrect $P_{s,set}$/$P_{r,set}$	The AHU supply/return air pressure setpoint is higher or lower than designed setpoint.	
F13	Incorrect HRW Control	The HRW control signal is incorrect.	
F14	Incorrect HCV Control	The heating coil valve signal is incorrect.	
F15	Incorrect Fan_s/Fan_r Control	The supply or return fan control signal is incorrect.	

Table A2
The symptom nodes in the proposed DBN

No.	Symptom	Rule	Symptom Type
S1	Comparing T_i and T_o	$\lvert T_i - T_o \rvert > \varepsilon_1$	Balance
S2	Supply fan alert is present	$A_{s,fan} = 1$	Additional
S3	Comparing $U_{s,\ fan}$, $P_{s,set}$ and P_s	$U_{s,fan} < 0\%$ or $U_{s,fan} > 100\%$ or ($U_{s,fan} < 100\%$ and $P_s < P_{s,set} - \varepsilon_2$) or ($U_{s,fan} > 0\%$ and $P_s > P_{s,set} + \varepsilon_2$)	Operational State
S4	Difference $P_{s,set}$ and P_s	$\lvert P_s - P_{s,set} \rvert > \varepsilon_3$	Operational State
S5	Return fan alert is present	$A_{r,fan} = 1$	Additional
S6	Comparison $U_{r,\ fan}$, $P_{r,set}$ and P_r	$U_{r,fan} < 0\%$ or $U_{r,fan} > 100\%$ or ($U_{r,fan} < 100\%$ and $P_r < P_{r,set} - \varepsilon_2$) or ($U_{r,fan} > 0\%$ and $P_r > P_{r,set} + \varepsilon_2$)	Operational State
S7	Difference $P_{r,set}$ *and* P_r	$\lvert P_r - P_{r,set} \rvert > \varepsilon_3$	Operational State
S8	High or low $P_{s,set}$	$\lvert P_{s,set} - 185 \rvert > \varepsilon_4$	Operational State
S9	High or low $P_{r,set}$	$\lvert P_{r,set} - 200 \rvert > \varepsilon_4$	Operational State
S10	High $\Delta\ P_s$	$\Delta P_s > \varepsilon_{5s}$	Operational State
S11	Supply filter alert present	$A_{s,filter} = 1$	Additional
S12	High $\Delta\ P_r$	$\Delta P_r > \varepsilon_{5r}$	Operational State
S13	Return filter alert present	$A_{r,filter} = 1$	Additional
S14	Low $\Delta\ P_s$	$U_{s,fan} \geq 5$ and $\Delta P_s < \varepsilon_6$	Operational State
S15	Low $\Delta\ P_r$	$U_{r,fan} \geq 5$ and $\Delta P_r < \varepsilon_6$	Operational State
S16	Comparing T_i *and* T_o	$\lvert T_o - T_i \rvert > \varepsilon_7$ or $T_i = NaN$ or $T_i < \varepsilon_{14}$ or $T_i > \varepsilon_{15}$	Balance

(*continued on next page*)

Table A2 (*continued*)

No.	Symptom	Rule	Symptom Type
S17	Comparing T_p *and* T_i when HRW off	$(\lvert T_p - T_i \rvert > \varepsilon_7$ and $U_{hrw} = 0\%)$ or $T_p = NaN$ or $T_p < \varepsilon_{14}$ or $T_p > \varepsilon_{15}$	Balance
S18	Comparing T_s *and* T_p when HCV closed	$(\lvert T_p - T_s \rvert > \varepsilon_7$ and $U_{hcv} = 0\%$ and $U_{ccv} = 0\%)$ or $T_s = NaN$ or $T_s < \varepsilon_{14}$ or $T_s > \varepsilon_{15}$	Balance
S19	T_r outlier or missing data	$T_r = NaN$ or $T_r < \varepsilon_{14}$ or $T_r > \varepsilon_{15}$	Operational State
S20	T_e outlier or missing data	$T_e = NaN$ or $T_e < \varepsilon_{14}$ or $T_e > \varepsilon_{15}$	Operational State
S21	Difference T_r *and* T_e with HRW off	$\lvert T_e - T_r \rvert > \varepsilon_7$ and $U_{hrw} = 0\%$	Balance
S22	Comparing U_{hcv}, T_s and T_{set}	$(U_{hcv} > 0\%$ and $T_s > T_{set} + \varepsilon_8)$ or $(U_{hcv} < 100\%$ and $T_s < T_{set} - \varepsilon_8)$ or $(U_{hcv} > 0\%$ and $U_{hrw} < 100\%)$ or $U_{hcv} < 0\%$ or $U_{hcv} > 100\%$	Operational State
S23	Difference T_s *and* T_{set}	$\lvert T_s - T_{set} \rvert > \varepsilon_9$	Operational State
S24	HCP alert present	$A_{hcp} = 1$	Additional
S25	Low heating coil efficiency	$(T_s - T_p) > \varepsilon_{10} * \frac{U_{hcv}}{100}$ and $U_{hcv} > 0\%$	Energy Performance
S26	Comparing T_p *and* T_s with HCV closed	$U_{hcv} = 0\%$ and $T_s > T_p + \varepsilon_{11}$	Balance
S27	Comparing U_{hrw}, T_s *and* T_{set}	$(U_{hrw} < 100\%$ and $T_s < T_{set} - \varepsilon_8$ and $T_r > T_o)$ or $(U_{erw} > 0\%$ and $T_r < T_o)$ or $(U_{erw} > 0\%$ and $T_s > T_{set} + \varepsilon_{12})$ or $U_{erw} < 0\%$ or $U_{erw} > 100\%$	Operational State
S28	Low HRW efficiency	$U_{hrw} > 0\%$ and $\frac{T_r - T_e}{T_r - T_i} < \varepsilon_{13} * \frac{U_{hrw}}{100}$	Energy Performance
S29	HRW alert present	$A_{hrw} = 1$	Additional
S30	P_s outlier or missing data	$P_s = NaN$ or $p_s < \varepsilon_{16}$ or $P_s > \varepsilon_{17}$	Operational State
S31	P_r outlier or missing data	$P_r = NaN$ or $P_r < \varepsilon_{16}$ or $P_r > \varepsilon_{17}$	Operational State
S32	ΔP_s outlier or missing data	$\Delta P_s = NaN$ or $\Delta P_s < \varepsilon_{16}$ or $\Delta P_s > \varepsilon_{17}$	Operational State
S33	ΔP_r outlier or missing data	$\Delta P_r = NaN$ or $\Delta P_r < \varepsilon_{16}$ or $\Delta P_r > \varepsilon_{17}$	Operational State
S34	High or low T_{set}	$T_{set} < \varepsilon_{18}$ or $T_{set} > \varepsilon_{19}$	Operational State
S35	Comparing U_{hcv} and U_{hrw}	$U_{hcv} > 0\%$ and $U_{hrw} < 100\%$	Operational State

*NaN means missing value.

Table A3
The thresholds in the symptoms

Threshold	Value	Threshold	Value
ε_1	2 °C	ε_{10}	5 °C
ε_2	5 Pa	ε_{11}	1 °C
ε_3	5 Pa	ε_{12}	1 °C
ε_4	1 Pa	ε_{13}	0.49
ε_{5s}	239 Pa	ε_{14}	−25 °C
ε_{5r}	174 Pa	ε_{15}	50 °C
ε_6	5 Pa	ε_{16}	0 Pa
ε_7	1 °C	ε_{17}	500 Pa
ε_8	1 °C	ε_{18}	19 °C
ε_9	1 °C	ε_{19}	22 °C

Data availability

Data will be made available on request.

References

[1] Eurostat, Shedding light on energy in the EU. https://doi.org/10.2785/405482, 2023.
[2] C. Maduta, D. D'Agostino, Readiness of zero-emission buildings (ZEBs) implementation in the European Union, in: M. Noro, C. Zilio (Eds.), E3S Web of Conferences, 2024 04009, https://doi.org/10.1051/e3sconf/202452304009.
[3] G. Martinopoulos, K.T. Papakostas, A.M. Papadopoulos, A comparative review of heating systems in EU countries, based on efficiency and fuel cost, Renew. Sustain. Energy Rev. 90 (2018) 687–699, https://doi.org/10.1016/j.rser.2018.03.060.
[4] C. Lu, S. Li, Z. Lu, Building energy prediction using artificial neural networks: a literature survey, Energy Build. 262 (2022), https://doi.org/10.1016/j.enbuild.2021.111718.
[5] S. Gopalan, A. Rijs, S. Chitkara, A. Thamban, R. Kramer, Fault prioritisation for air handling units using fault modelling and actual fault occurrence data, Energy Build. 319 (2024) 114476, https://doi.org/10.1016/j.enbuild.2024.114476.
[6] B. Gunay, B.W. Hobson, D. Darwazeh, J. Bursill, Estimating energy savings from HVAC controls fault correction through inverse greybox model-based virtual metering, Energy Build. 282 (2023), https://doi.org/10.1016/j.enbuild.2023.112806.
[7] Y. Zhao, T. Li, X. Zhang, C. Zhang, Artificial intelligence-based fault detection and diagnosis methods for building energy systems: advantages, challenges and the future, Renew. Sustain. Energy Rev. 109 (2019) 85–101, https://doi.org/10.1016/j.rser.2019.04.021.
[8] Z. Chen, Z. O'Neill, J. Wen, O. Pradhan, T. Yang, X. Lu, G. Lin, S. Miyata, S. Lee, C. Shen, R. Chiosa, M.S. Piscitelli, A. Capozzoli, F. Hengel, A. Kührer, M. Pritoni, W. Liu, J. Clauß, Y. Chen, T. Herr, A review of data-driven fault detection and diagnostics for building HVAC systems, Appl. Energy 339 (2023), https://doi.org/10.1016/j.apenergy.2023.121030.

[9] J. Chen, L. Zhang, Y. Li, Y. Shi, X. Gao, Y. Hu, A review of computing-based automated fault detection and diagnosis of heating, ventilation and air conditioning systems, Renew. Sustain. Energy Rev. 161 (2022) 112395, https://doi.org/10.1016/j.rser.2022.112395.
[10] Z. Shi, W. O'Brien, Development and implementation of automated fault detection and diagnostics for building systems: a review, Autom. ConStruct. 104 (2019) 215–229, https://doi.org/10.1016/j.autcon.2019.04.002.
[11] K. Heimar Andersen, S. Pommerencke Melgaard, H. Johra, A. Marszal-Pomianowska, R. Lund Jensen, P. Kvols Heiselberg, Barriers and drivers for implementation of automatic fault detection and diagnosis in buildings and HVAC systems: an outlook from industry experts, Energy Build. 303 (2024) 113801, https://doi.org/10.1016/j.enbuild.2023.113801.
[12] S. Frank, X. Jin, D. Studer, A. Farthing, Assessing barriers and research challenges for automated fault detection and diagnosis technology for small commercial buildings in the United States, Renew. Sustain. Energy Rev. 98 (2018) 489–499, https://doi.org/10.1016/j.rser.2018.08.046.
[13] C. Fan, Q. Wu, Y. Zhao, L. Mo, Integrating active learning and semi-supervised learning for improved data-driven HVAC fault diagnosis performance, Appl. Energy 356 (2024) 122356, https://doi.org/10.1016/j.apenergy.2023.122356.
[14] C. Lu, J. Gu, W. Lu, An improved attention-based deep learning approach for robust cooling load prediction: public building cases under diverse occupancy schedules, Sustain. Cities Soc. 96 (2023), https://doi.org/10.1016/j.scs.2023.104679.
[15] D. Lee, C.-W. Lai, K.-K. Liao, J.-W. Chang, Artificial intelligence assisted false alarm detection and diagnosis system development for reducing maintenance cost of chillers at the data centre, J. Build. Eng. 36 (2021) 102110, https://doi.org/10.1016/j.jobe.2020.102110.
[16] T. Li, Y. Zhou, Y. Zhao, C. Zhang, X. Zhang, A hierarchical object oriented Bayesian network-based fault diagnosis method for building energy systems, Appl. Energy 306 (2022), https://doi.org/10.1016/j.apenergy.2021.118088.
[17] C. Lu, Z. Wang, M. Mosteiro-Romero, L. Itard, Diagnostic Bayesian network in building energy systems: current insights, practical challenges, and future trends, Energy Build. 341 (2025) 115845, https://doi.org/10.1016/j.enbuild.2025.115845.
[18] A. Taal, L. Itard, W. Zeiler, A reference architecture for the integration of automated energy performance fault diagnosis into HVAC systems, Energy Build. 179 (2018) 144–155, https://doi.org/10.1016/j.enbuild.2018.08.031.
[19] Y. Zhao, J. Wen, F. Xiao, X. Yang, S. Wang, Diagnostic Bayesian networks for diagnosing air handling units faults – part I: faults in dampers, fans, filters and sensors, Appl. Therm. Eng. 111 (2017), https://doi.org/10.1016/j.applthermaleng.2015.09.121.
[20] Y. Zhao, J. Wen, S. Wang, Diagnostic Bayesian networks for diagnosing air handling units faults - part II: faults in coils and sensors, Appl. Therm. Eng. 90 (2015), https://doi.org/10.1016/j.applthermaleng.2015.07.001.
[21] Z. Wang, C. Lu, A. Taal, S. Gopalan, K. Mohammed, A. Meijer, L. Itard, Bayesian network-based fault detection and diagnosis of heating components in heat recovery ventilation, in: The 17th RoomVent Conference, 2024. Stockholm.
[22] A. Taal, L. Itard, P&ID-based automated fault identification for energy performance diagnosis in HVAC systems: 4S3F method, development of DBN models and application to an ATES system, Energy Build. 224 (2020), https://doi.org/10.1016/j.enbuild.2020.110289.
[23] A. Taal, L. Itard, Thr, Autom. ConStruct. 119 (2020), https://doi.org/10.1016/j.autcon.2020.103344.
[24] M. Mosteiro-Romero, Z. Wang, C. Lu, L. Itard, Whole-building HVAC fault detection and diagnosis with the 4S3F method: towards integrating systems and occupant feedback, in: The 5th Asia Conference of International Building Performance Simulation Association 2024, 2024. Osaka, Japan.
[25] M. Hu, H. Chen, L. Shen, G. Li, Y. Guo, H. Li, J. Li, W. Hu, A machine learning bayesian network for refrigerant charge faults of variable refrigerant flow air conditioning system, Energy Build. 158 (2018) 668–676, https://doi.org/10.1016/j.enbuild.2017.10.012.
[26] Z. Wang, L. Wang, Y. Tan, J. Yuan, X. Li, Fault diagnosis using fused reference model and Bayesian network for building energy systems, J. Build. Eng. 34 (2021), https://doi.org/10.1016/j.jobe.2020.101957.
[27] T. Li, Y. Zhao, C. Zhang, J. Luo, X. Zhang, A knowledge-guided and data-driven method for building HVAC systems fault diagnosis, Build. Environ. 198 (2021), https://doi.org/10.1016/j.buildenv.2021.107850.
[28] D. Wu, H. Yang, K. Xu, X. Meng, S. Yin, C. Zhu, X. Jin, Data and knowledge fusion-driven Bayesian networks for interpretable fault diagnosis of HVAC systems, Int. J. Refrig. (2024), https://doi.org/10.1016/j.ijrefrig.2024.02.019.
[29] Z. Wang, B. Liang, J.J. Guo, L. Wang, Y. Tan, X. Li, Fault diagnosis based on residual–knowledge–data jointly driven method for chillers, Eng. Appl. Artif. Intell. 125 (2023), https://doi.org/10.1016/j.engappai.2023.106768.
[30] Z. Wang, Z. Wang, X. Gu, S. He, Z. Yan, Feature selection based on Bayesian network for chiller fault diagnosis from the perspective of field applications, Appl. Therm. Eng. 129 (2018), https://doi.org/10.1016/j.applthermaleng.2017.10.079.
[31] L.K. Norford, J.A. Wright, R.A. Buswell, D. Luo, C.J. Klaassen, A. Suby, Demonstration of fault detection and diagnosis methods for air-handling units, HVAC R Res. 8 (2002) 41–71, https://doi.org/10.1080/10789669.2002.10391289.
[32] J. Kim, Y. Kwak, S.-H. Mun, J.-H. Huh, Imputation of missing values in residential building monitored data: energy consumption, behavior, and environment information, Build. Environ. 245 (2023) 110919, https://doi.org/10.1016/j.buildenv.2023.110919.
[33] C. Fu, M. Quintana, Z. Nagy, C. Miller, Filling time-series gaps using image techniques: multidimensional context autoencoder approach for building energy data imputation, Appl. Therm. Eng. 236 (2024) 121545, https://doi.org/10.1016/j.applthermaleng.2023.121545.
[34] T.I. Salsbury, R.C. Diamond, Fault detection in HVAC systems using model-based feedforward control, Energy Build. 33 (2001) 403–415, https://doi.org/10.1016/S0378-7788(00)00122-5.
[35] E. Halmetoja, H. Salonen, H. Ihasalo, K. Främling, Critical study of the applicability of additional IAQ sensors in older buildings, Intell. Build. Int. 14 (2022) 753–765, https://doi.org/10.1080/17508975.2021.2011702.
[36] L. Chamari, E. Petrova, P. Pauwels, An end-to-end implementation of a service-oriented architecture for data-driven smart buildings, IEEE Access 11 (2023) 117261–117281, https://doi.org/10.1109/ACCESS.2023.3325767.
[37] O. Nehasil, L. Dobiášová, V. Mazanec, J. Široký, Versatile AHU fault detection – design, field validation and practical application, Energy Build. 237 (2021) 110781, https://doi.org/10.1016/j.enbuild.2021.110781.
[38] H.H. Hosamo, P.R. Svennevig, K. Svidt, D. Han, H.K. Nielsen, A digital twin predictive maintenance framework of air handling units based on automatic fault detection and diagnostics, Energy Build. 261 (2022) 111988, https://doi.org/10.1016/j.enbuild.2022.111988.
[39] X. Xie, J. Merino, N. Moretti, P. Pauwels, J.Y. Chang, A. Parlikad, Digital twin enabled fault detection and diagnosis process for building HVAC systems, Autom. ConStruct. 146 (2023) 104695, https://doi.org/10.1016/j.autcon.2022.104695.
[40] Y. Chen, J. Wen, O. Pradhan, L.J. Lo, T. Wu, Using discrete Bayesian networks for diagnosing and isolating cross-level faults in HVAC systems, Appl. Energy 327 (2022), https://doi.org/10.1016/j.apenergy.2022.120050.
[41] J. Wen, L. Shun, Tools for Evaluating Fault Detection and Diagnostic Methods for air-handling Units, 2011.
[42] L. Schibuola, C. Tambani, Performance comparison of heat recovery systems to reduce viral contagion in indoor environments, Appl. Therm. Eng. 190 (2021) 116843, https://doi.org/10.1016/j.applthermaleng.2021.116843.
[43] K.-P. Lee, B.-H. Wu, S.-L. Peng, Deep-learning-based fault detection and diagnosis of air-handling units, Build. Environ. 157 (2019) 24–33, https://doi.org/10.1016/j.buildenv.2019.04.029.
[44] M. Elnour, N. Meskin, M. Al-Naemi, Sensor data validation and fault diagnosis using auto-associative neural network for HVAC systems, J. Build. Eng. 27 (2020) 100935, https://doi.org/10.1016/j.jobe.2019.100935.
[45] K. Yan, A. Chong, Y. Mo, Generative adversarial network for fault detection diagnosis of chillers, Build. Environ. 172 (2020) 106698, https://doi.org/10.1016/j.buildenv.2020.106698.
[46] A. Taal, L. Itard, Fault detection and diagnosis for indoor air quality in DCV systems: application of 4S3F method and effects of DBN probabilities, Build. Environ. 174 (2020), https://doi.org/10.1016/j.buildenv.2019.106632.
[47] G. Li, Q. Yao, C. Fan, C. Zhou, G. Wu, Z. Zhou, X. Fang, An explainable one-dimensional convolutional neural networks based fault diagnosis method for building heating, ventilation and air conditioning systems, Build. Environ. 203 (2021) 108057, https://doi.org/10.1016/j.buildenv.2021.108057.
[48] S. Taheri, A. Ahmadi, B. Mohammadi-Ivatloo, S. Asadi, Fault detection diagnostic for HVAC systems via deep learning algorithms, Energy Build. 250 (2021) 111275, https://doi.org/10.1016/j.enbuild.2021.111275.

[49] C. Fan, Y. Liu, X. Liu, Y. Sun, J. Wang, A study on semi-supervised learning in enhancing performance of AHU unseen fault detection with limited labeled data, Sustain. Cities Soc. 70 (2021) 102874, https://doi.org/10.1016/j.scs.2021.102874.
[50] X. Lei, Y. Chen, M. Bergés, B. Akinci, Formalized control logic fault definition with ontological reasoning for air handling units, Autom. ConStruct. 129 (2021) 103781, https://doi.org/10.1016/j.autcon.2021.103781.
[51] B. Wu, W. Cai, F. Cheng, H. Chen, Simultaneous-fault diagnosis considering time series with a deep learning transformer architecture for air handling units, Energy Build. 257 (2022) 111608, https://doi.org/10.1016/j.enbuild.2021.111608.
[52] J. Huang, J. Wen, H. Yoon, O. Pradhan, T. Wu, Z. O'Neill, K. Selcuk Candan, Real vs. simulated: questions on the capability of simulated datasets on building fault detection for energy efficiency from a data-driven perspective, Energy Build. 259 (2022) 111872, https://doi.org/10.1016/j.enbuild.2022.111872.
[53] K. Yan, J. Su, J. Huang, Y. Mo, Chiller fault diagnosis based on VAE-enabled generative adversarial networks, IEEE Trans. Autom. Sci. Eng. 19 (2022) 387–395, https://doi.org/10.1109/TASE.2020.3035620.
[54] F.N. Irani, M. Bakhtiaridoust, M. Yadegar, N. Meskin, A data-driven approach for fault diagnosis in multi-zone HVAC systems: deep neural bilinear koopman parity, J. Build. Eng. 76 (2023) 107127, https://doi.org/10.1016/j.jobe.2023.107127.
[55] Y. Gao, S. Miyata, Y. Akashi, How to improve the application potential of deep learning model in HVAC fault diagnosis: based on pruning and interpretable deep learning method, Appl. Energy 348 (2023) 121591, https://doi.org/10.1016/j.apenergy.2023.121591.
[56] Y. Gao, S. Miyata, Y. Akashi, Automated fault detection and diagnosis of chiller water plants based on convolutional neural network and knowledge distillation, Build. Environ. 245 (2023) 110885, https://doi.org/10.1016/j.buildenv.2023.110885.
[57] K. Yan, X. Chen, X. Zhou, Z. Yan, J. Ma, Physical model informed fault detection and diagnosis of air handling units based on transformer generative adversarial network, IEEE Trans. Ind. Inf. 19 (2023) 2192–2199, https://doi.org/10.1109/TII.2022.3193733.
[58] Z. Chen, F. Xiao, F. Guo, Similarity learning-based fault detection and diagnosis in building HVAC systems with limited labeled data, Renew. Sustain. Energy Rev. 185 (2023) 113612, https://doi.org/10.1016/j.rser.2023.113612.
[59] Y. Yan, J. Cai, Y. Tang, L. Chen, Fault diagnosis of HVAC AHUs based on a BP-MTN classifier, Build. Environ. 227 (2023) 109779, https://doi.org/10.1016/j.buildenv.2022.109779.
[60] H. Zhang, W. Yang, W. Yi, J.B. Lim, Z. An, C. Li, Imbalanced data based fault diagnosis of the chiller via integrating a new resampling technique with an improved ensemble extreme learning machine, J. Build. Eng. 70 (2023) 106338, https://doi.org/10.1016/j.jobe.2023.106338.
[61] Z. Du, X. Liang, S. Chen, X. Zhu, K. Chen, X. Jin, Knowledge-infused deep learning diagnosis model with self-assessment for smart management in HVAC systems, Energy 263 (2023) 125969, https://doi.org/10.1016/j.energy.2022.125969.
[62] H.H. Hosamo, H.K. Nielsen, D. Kraniotis, P.R. Svennevig, K. Svidt, Digital twin framework for automated fault source detection and prediction for comfort performance evaluation of existing non-residential Norwegian buildings, Energy Build. 281 (2023) 112732, https://doi.org/10.1016/j.enbuild.2022.112732.
[63] J. Huang, N. Ghalamsiah, A. Patharkar, O. Pradhan, M. Chu, T. Wu, J. Wen, Z. O'Neill, K. Selcuk Candan, An entropy-based causality framework for cross-level faults diagnosis and isolation in building HVAC systems, Energy Build. 317 (2024) 114378, https://doi.org/10.1016/j.enbuild.2024.114378.
[64] M. Babadi Soultanzadeh, M.M. Ouf, M. Nik-Bakht, P. Paquette, S. Lupien, Fault detection and diagnosis in light commercial buildings' HVAC systems: a comprehensive framework, application, and performance evaluation, Energy Build. 316 (2024) 114341, https://doi.org/10.1016/j.enbuild.2024.114341.
[65] Z. Wang, J. Guo, P. Xia, L. Wang, C. Zhang, Q. Leng, K. Zheng, Feature selection for chillers fault diagnosis from the perspectives of machine learning and field application, Energy Build. 307 (2024) 113937, https://doi.org/10.1016/j.enbuild.2024.113937.
[66] W. Yang, H. Zhang, J.B. Lim, Y. Zhang, H. Meng, A new chiller fault diagnosis method under the imbalanced data environment via combining an improved generative adversarial network with an enhanced deep extreme learning machine, Eng. Appl. Artif. Intell. 137 (2024) 109218, https://doi.org/10.1016/j.engappai.2024.109218.
[67] H. Zhang, Y. Zhang, H. Meng, J.B. Lim, W. Yang, A novel global modelling strategy integrated dynamic kernel canonical variate analysis for the air handling unit fault detection via considering the two-directional dynamics, J. Build. Eng. 96 (2024) 110402, https://doi.org/10.1016/j.jobe.2024.110402.
[68] T. Gao, S. Marié, P. Béguery, S. Thebault, S. Lecoeuche, Integrated building fault detection and diagnosis using data modeling and Bayesian networks, Energy Build. 306 (2024), https://doi.org/10.1016/j.enbuild.2024.113889.
[69] M.C. Comstock, J.E. Braun, Fault Detection and Diagnostic (FDD) Requirements and Evaluation Tools for Chillers, 2002. West Lafayette.
[70] V. Moudgil, K. Hewage, S.A. Hussain, R. Sadiq, Integration of IoT in building energy infrastructure: a critical review on challenges and solutions, Renew. Sustain. Energy Rev. 174 (2023) 113121, https://doi.org/10.1016/j.rser.2022.113121.
[71] M. Lillstrang, M. Harju, G. del Campo, G. Calderon, J. Röning, S. Tamminen, Implications of properties and quality of indoor sensor data for building machine learning applications: two case studies in smart campuses, Build. Environ. 207 (2022) 108529, https://doi.org/10.1016/j.buildenv.2021.108529.
[72] D. Koller, N. Friedman, Probabilistic Graphical Models- Principles and Techniques, 1989.
[73] N. Djuric, V. Novakovic, Review of possibilities and necessities for building lifetime commissioning, Renew. Sustain. Energy Rev. 13 (2009) 486–492, https://doi.org/10.1016/j.rser.2007.11.007.
[74] S. Yoon, Virtual sensing in intelligent buildings and digitalization, Autom. ConStruct. 143 (2022) 104578, https://doi.org/10.1016/j.autcon.2022.104578.
[75] Apache Kafka, Apache kafka documentation. https://kafka.apache.org/documentation/, 2024. (Accessed 18 December 2024).
[76] Apache ZooKeeper, Apache Zookeeper Document, 2024 (n.d.). https://zookeeper.apache.org/(accessed December 18, 2024).
[77] Influxdb, Influxdb Document, 2024 (n.d.). https://docs.influxdata.com/influxdb/v2/(accessed December 18, 2024).
[78] C. Lu, Z. Wang, M. Mosteiro-Romero, L. Itard, Introducing causality to symptom baseline estimation: a critical case study in fault detection of building energy systems, in: The 5th Asia Conference of International Building Performance Simulation Association 2024, 2024. Osaka, Japan.